Vibro-Acoustic Source Localization Using the Transmissibility Concept

Duarte Pereira
duarte.pereira@tecnico.ulisboa.pt
Instituto Superior Técnico, Universidade de Lisboa, Portugal

January 2021

Abstract

This work focuses on the study of vibro-acoustic responses using the transmissibility concept with the purpose of identifying vibro-acoustic sources. To do so, numerical methodologies developed by previous authors are updated to obtain transmissibility functions in structural, acoustic and vibro-acoustic systems with lower computational effort. Additionally, this work features experimental procedures to estimate responses in acoustic and vibro-acoustic systems.

The numerical methodologies use the finite element method (FEM) (implemented in commercial software ANSYS) to discretize the system. Then, the global matrices are imported to Matlab®, where the transmissibility functions are estimated. Using the transmissibility concept, a Matlab® routine is created to perform source localization in vibro-acoustic systems. The experimental procedures allow evaluating the proximity to the numerical models, as well as determining how these models may be updated.

In conclusion, it is intended that the developed methodologies and obtained results present a contribution to the field of vibro-acoustic transmissibility, which is still relatively undeveloped.
Keywords: Vibro-Acoustics, Transmissibility Concept, Source Localization, Finite Element Method, Computational Effort

1 Introduction

Despite recent advances in the area of vibro-acoustic transmissibility, this concept remains quite undeveloped [1]. In this work, one intends to study not only steady state responses and transmissibility functions in the frequency domain, but also the use of the transmissibility concept and its properties to conduct source localization in vibro-acoustic systems.

The concept of transmissibility in single degree of freedom (SDOF) systems is well known and has been widely spread in literature concerning vibration. However, the concept of multiple degree of freedom (MDOF) transmissibility is more recent. The concept of MDOF transmissibility in mass-spring systems is described in [2]. Transmissibility in mass-spring MDOF systems is also present in [3], in which the source identification problem is also discussed. This concept is then generalized to continuous structural systems, as discussed in [4], in which are proposed both numerical and experimental methods to evaluate transmissibility in a simply supported beam. More recently, the concept of MDOF transmissibility was applied to acoustic systems. In [5], the transmissibility concept is applied to acoustic systems by using it, not only to estimate pressure responses in acoustic domains, but also to perform the localization of acoustic sources in simplified aircraft models. This is done by using a combined approach of the FEM (with ANSYS APDL [6]) and Matlab® to estimate transmissibility functions, a methodologie that is used in the present work.

The concept of vibro-acoustic transmissibility as well as its importance in operational transfer path analysis (OTPA) is introduced in [7], and in [1] is developed a methodology for obtaining transmissibility functions in coupled vibro-acoustic systems with fluid structure interactions (FSI).

In the present work, the author takes on the methodologies developed in [1, 5], and updates them to evaluate vibro-acoustic transmissibility with lower computational effort. Therefore, the main objectives of this work are:

- Use transmissibility functions to estimate pressures (unknown pressures) in a vibro-acoustic

system for a given measured displacement (known displacements) in the structure. This is useful since some of these pressures are in places of difficult access;
- Reduce the computational effort required to extract the transmissibility functions in Matlab®;
- Evaluate the potential of the concept of vibro-acoustic transmissibility to perform source localization in coupled vibro-acoustic systems.

The numerical approach is based on the FEM, implemented in ANSYS APDL. The models are developed in ANSYS, and the globally assembled matrices are imported to Matlab®, where the transmissibility matrices are computed. The source localization algorithm is also implemented in Matlab® using the estimated transmissibility functions. The experimental model is based on the procedures developed in [8], and is used to obtain acoustic and vibro-acoustic responses in a wooden cavity. The experimental results are compared with the numerical ones to assess the amount of further updating required in these models.

Throughout the following sections, the most relevant theoretical fundamentals are presented, the implemented methodologies are briefly described, and the results are presented along with a critical discussion. To conclude, some final remarks and conclusions are presented based on the results obtained.

2 Theoretical Background

This section contains the fundamentals concerning vibration, acoustics and vibro-acoustics, including the theory related to the transmissibility concept.

2.1 Vibration in MDOF systems

The general differential equation for vibration in steady-state MDOF systems may be written for a displacement $\{x(t)\}$, and an applied load $\{f(t)\}$, in the time domain, as

$$[M]\{\ddot{x}(t)\} + [C]\{\dot{x}(t)\} + [K]\{x(t)\} = \{f(t)\} \quad (2.1)$$

or, in the frequency domain, considering harmonic displacements and loads, as

$$(-\omega^2[M] + i\omega[C] + [K])\{X\} = \{F\} \quad (2.2)$$

where $[K]$, $[C]$ and $[M]$ are the stiffness, damping, and mass matrices respectively, $\{X\}$ is the vector of complex displacement amplitudes, and $\{F\}$ is the vector of complex load amplitudes. The dynamic stiffness matrix $[Z]$ is given by $-\omega^2[M]+i\omega[C]+[K]$, and its inverse is the receptance matrix $[H]$.

2.2 Acoustic Waves

Combining the equations of mass and momentum conservation (see [9]), and considering that for plane waves $p = c^2\rho$, one can obtain the 3D wave equation:

$$\frac{1}{c^2}\frac{\partial^2 p}{\partial t^2} - \nabla^2 p = 0 \quad (2.3)$$

where c is the sound speed and p is the pressure of the disturbance.

A dynamic acoustic system in steady state may also be modelled, in the frequency domain, by a differential equation [5]. This equation is similar to equation 2.2 and may be expressed as

$$(-\omega^2[M] + i\omega[C] + [K])\{P\} = \{Q\} \quad (2.4)$$

where $[M]$, $[C]$ and $[K]$ are the acoustic mass, damping, and stiffness matrices respectively, $\{P\}$ is the vector of complex pressure amplitudes, and $\{Q\}$ is the vector of volume accelerations. Similarly to the vibration problem, one can define the dynamic stiffness matrix and the receptance matrix for an acoustic system.

2.3 The Transmissibility Concept

The transmissibility concept may be established in solid structures by defining a vector of harmonically applied loads F_A at coordinates A, a vector of unknown response amplitudes X_U at coordinates U, and a vector of known response amplitudes X_K at coordinates K. Thus, one may write, in terms of the receptance matrix [2]:

$$X_U = H_{UA}F_A \quad (2.5)$$

$$X_K = H_{KA}F_A \quad (2.6)$$

then, eliminating F_A from the previous equation, one obtains

$$X_U = H_{UA}H_{KA}^{+}X_K \quad (2.7)$$

and the displacement transmissibility matrix can be defined as follows.

$$T_{UK}^{(A)} = H_{UA}H_{KA}^{+} \quad (2.8)$$

For evaluating transmissibility of forces in solid structures, one has to consider the vectors of responses X_K and X_U, which correspond to the load vectors F_K and F_U respectively, along with X_C, the responses in the remaining coordinates. By doing so, one can write the following expression.

$$\begin{Bmatrix} X_K \\ X_U \\ X_C \end{Bmatrix} = \begin{bmatrix} H_{KK} & H_{KU} \\ H_{UK} & H_{UU} \\ H_{CK} & H_{CU} \end{bmatrix} \begin{Bmatrix} F_K \\ F_U \end{Bmatrix} \quad (2.9)$$

Assuming that the responses at the reaction coordinates X_U are zero, one can obtain the transmissibility matrix [2].

$$F_U = -H_{UU}^{-1}H_{UK}F_K \Rightarrow T_{UK} = -H_{UU}^{-1}H_{UK} \quad (2.10)$$

As an alternative, one may also use the dynamic stiffness matrix to determine the transmissibility matrix. Assuming the same sets of coordinates and vectors as in the previous case, but adding a vector of fictitious loads F_C, the following equation is obtained.

$$\begin{Bmatrix} F_K \\ F_C \\ F_U \end{Bmatrix} = \begin{bmatrix} Z_{KK} & Z_{KC} & Z_{KU} \\ Z_{CK} & Z_{CC} & Z_{CU} \\ Z_{UK} & Z_{UC} & Z_{UU} \end{bmatrix} \begin{Bmatrix} X_K \\ X_C \\ X_U \end{Bmatrix} \tag{2.11}$$

Then, considering $X_U = 0$ and defining

$$X_E = \begin{Bmatrix} X_K \\ X_C \end{Bmatrix}, F_E = \begin{Bmatrix} F_K \\ F_C \end{Bmatrix} \tag{2.12}$$

one can obtain the following equations [2].

$$F_U = Z_{UE} Z_{EE}^{-1} F_E \Rightarrow T_{UE} = Z_{UE} Z_{EE}^{-1} \tag{2.13}$$

The concept of transmissibility may be generalized to the field of acoustics. As before, by defining U as the set of unknown pressures, K as the set of known pressures, and C as the set of the remaining coordinates, one can write, as described in [5], in terms of the receptance matrix $[H]$:

$$\begin{Bmatrix} P_K \\ P_U \\ P_C \end{Bmatrix} = \begin{bmatrix} H_{KK} & H_{KU} \\ H_{UK} & H_{UU} \\ H_{CK} & H_{CU} \end{bmatrix} \begin{Bmatrix} Q_K \\ Q_U \end{Bmatrix} \tag{2.14}$$

and assuming no loads at coordinates C, by expanding the system of two equations, considering Q_K to be zero and solving for Q_U, one can obtain the following equation for an imposed pressure at set U [5].

$$P_K = H_{KU} H_{UU}^{-1} \overline{P}_U \Rightarrow T_{KU} = H_{KU} H_{UU}^{-1} \tag{2.15}$$

In this work, the concept of vibro-acoustic transmissibility is related to coupled vibro-acoustic systems. The finite element (FE) models for the unconstrained degrees of freedom (DOFs) concerning structural and acoustic systems, may be defined in terms of the global assembled matrices by equation 2.2 and 2.4, respectively. To obtain the coupled FE model, the coupling terms $[K_C\{p\}]$ (force loading of the acoustic pressure on the elastic shell) and $-\omega^2[M_C]\{u\}$ (continuity between normal shell velocity and normal fluid velocity is ensured by adding this term) must be added to the structural and acoustic FE models, respectively. Then, the coupled FE model for vibro-acoustic systems may be defined as [10],

$$\left(\begin{bmatrix} K_S & K_C \\ 0 & K_A \end{bmatrix} + i\omega \begin{bmatrix} C_S & 0 \\ 0 & C_A \end{bmatrix} - \omega^2 \begin{bmatrix} M_S & 0 \\ -\rho_0 K_C^T & M_A \end{bmatrix} \right) \begin{Bmatrix} u \\ p \end{Bmatrix} = \begin{Bmatrix} F_S \\ F_A \end{Bmatrix} \tag{2.16}$$

where the subscripts A, S and C correspond to the acoustic terms, structural terms, and coupling terms respectively.

Considering U and K, the sets of coordinates where the imposition is set and where the responses are measured respectively, the vibro-acoustic transmissibility may be defined in terms of the receptance matrix by writing the following equation [1].

$$\begin{Bmatrix} u_U \\ P_K \end{Bmatrix} = \begin{bmatrix} H_{UU} & H_{UK} \\ H_{KU} & H_{KK} \end{bmatrix} \begin{Bmatrix} F_U \\ F_K \end{Bmatrix} \tag{2.17}$$

Then, defining F_U as a function of u_U, and assuming that F_K is zero, one obtains the equation below.

$$P_K = H_{KU} H_{UU}^{-1} u_U \Rightarrow T_{KU}^{SF} = H_{KU} H_{UU}^{-1} \tag{2.18}$$

This case concerns a structural displacement imposition that leads to an acoustic pressure response. However, the case where an acoustic pressure imposition leads to a structural response may also occur. If so, the procedure to obtain the transmissibility matrix is the same and, therefore, one can write the following expression [1].

$$u_K = H_{KU} H_{UU}^{-1} P_U \Rightarrow T_{KU}^{FS} = H_{KU} H_{UU}^{-1} \tag{2.19}$$

3 Methodology

Here, the numerical and experimental methodologies used to model and obtain the results of the analysed systems are described. These systems include a mass-spring system, an acoustic tube, an acoustic tube with a plate in one end with FSI, an acoustic cavity, a vibro-acoustic cavity, and a simplified aircraft interior.

3.1 Numerical Models

3.1.1 Mass-spring system

This system is that presented in [2], and is used to evaluate force transmissibility. The goal is to obtain the transmissibility matrix between the fixed nodes and the nodes at which the loads are applied. The FE model is created in Matlab®, as described in [1], by introducing the global matrices and force vectors as an input. Then, a cycle is created to extract $[Z]$ and $[H]$ over a previously defined frequency range. The submatrices of $[Z]$ and $[H]$ are also created in the cycle (according to equations 2.10 and 2.13), with respect to the coordinates between which the transmissibility functions are to be determined. Finally, the computed transmissibilities are compared with those presented in [2], for verification purposes.

3.1.2 Acoustic and Vibro-acoustic Tube

Here, one intends to obtain the pressure distribution inside an acoustic tube, and compare it with

the analytical solutions available. Then, it is intended to conduct transmissibility analyses in both acoustic and vibro-acoustic tubes. The FE models concerning these tubes are implemented in ANSYS APDL, and are similar to the ones modelled in [1]. To do so, one begins by creating a square with a 0.1 m side. Then, a volume is created by extruding this square along 4 m in the normal direction. The mesh is then created using FLUID30 elements, and a 1 Pa pressure is imposed at one of the ends. The following material properties are considered for the acoustic fluid: the sound speed is 344 m/s; the mass density is 1.21 kg/m^3, and the boundary admittance is 0. Modal and harmonic analyses are conducted, and the pressure distribution inside the tube is compared with analytical solutions (see [11]) for verification purposes.

The global matrices are then imported to Matlab® to estimate unknown pressure responses using the transmissibility concept (equation 2.15), and a methodology similar to the one described in 3.1.1.

The vibro-acoustic tube has the same geometry and material properties as the acoustic tube. After meshing the acoustic tube, one has to insert a plate (SHELL181 elements) at one of the ends, and turn the elements that are touching the plate to FSI elements, as described in [12]. The plate is considered to have a longitudinal modulus of elasticity of 210 GPa, a mass density of 7800 kg/m^3, a Poisson ratio of 0.3, and a 1 mm thickness. Then, a 1 N load is applied at the center of the plate (along the normal direction to the plate), and the displacement and rotation DOFs are fixed along the plate's edges. Lastly, the modal and harmonic analyses are conducted, and the computed transmissibilities are compared with the ones obtained with Matlab® using the transmissibility concept (using the methodology described in 3.1.1). In this case, equation 2.18 must be modified, as described later in section 3.3.

3.1.3 Acoustic and Vibro-acoustic Cavities

The main objective of these analyses is to numerically obtain the pressure responses at some coordinates, and to compare them with experimental results. In the case of the vibro-acoustic cavity, an algorithm is implemented to perform source identification. The models of the cavities are also created in ANSYS APDL. The acoustic cavity is modelled as a 2D domain, and the vibro-acoustic cavity as a 3D system. To create the geometry of these models, one has to create several keypoints at the coordinates of the cavity's vertices. Then, lines are created to connect all the keypoints, and an area is created within those lines. In the case of the vibro-acoustic cavity, the area is extruded along the normal direction to the intended height (0.1 m). The meshes are then created with 0.025 m FLUID29 elements for the acoustic cavity, and 0.05 m FLUID30 elements for the vibro-acoustic cavity. The shell is inserted in the vibro-acoustic cavity (SHELL181 elements), and the displacement and rotation DOFs are fixed around the edges of the plate. The elements touching the shell are made FSI elements. The acoustic fluid has the same properties as the fluid in the acoustic tube, and the plate has a 205 GPa longitudinal modulus of elasticity, a mass density of 7800 kg/m^3, a thickness of 1 mm, and a Poisson ratio of 0.3. The unitary pressures are then imposed in the 2D acoustic cavity, and the 1 N harmonic load is applied to the plate (along the normal direction to the plate) in the 3D vibro-acoustic cavity. A harmonic and a modal analyses are conducted, and the results of the 2D cavity are compared with the results obtained experimentally. The results of the vibro-acoustic harmonic analysis are compared with the ones obtained using the transmissibility concept in order to perform the identification of sources. The Matlab® routines used to obtain transmissibility functions are similar to the ones described in 3.1.1. The methodology used in the source localization problem is described in section 3.3. The dimensions and specifications of both these cavities are presented in 3.2.

3.1.4 Simplified Aircraft Interior

In this example, it is intended to estimate unknown pressures at certain locations using both the FEM and the transmissibility concept, for a given imposed displacement on the elastic shell. It is also intended to use the transmissibility concept to perform source identification. To create this model, a half circle with a radius of 2.5 m is defined and extruded along the normal direction for 3 m, making a half cylinder with a 2.5 m radius and 3 m long.

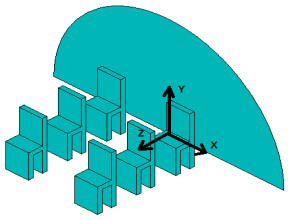

Figure 3.1: Model of the aircraft interior.

Six chairs are then modelled with a 1.25 m height, a 0.1 m thickness on the back, legs and sit. The height of the sit is 0.6 m, and the length and width are 0.4 m and 0.5 m respectively. The chairs have a longitudinal space of 0.45 m along them, and their side distance is 1 m. There are two rows of 3 chairs in each side of the cabin. A schematic of the aircraft's

interior geometry is presented in figure 3.1.

Then, the mesh is created using FLUID30 elements with a maximum length of 0.25 m. A shell is inserted around the entire fluid domain (1 source case), or only on the two vertical walls (2 sources case), and the elements touching the plates are turned to FSI. In this case, all the boundaries are considered to be reflective, and the loads are applied on the walls/floor along the direction normal to those surfaces. The loads are applied at coordinates (0;0;1.5) m (case with 1 source), and at coordinates (0;1.35;3) m and (0;1.35;0) m (case with 2 sources). The coordinates of these points are related to the coordinate axes in figure 3.1. The material properties of the acoustic fluid are the same as in the previous cases, and the shell has a longitudinal modulus of elasticity of 205 GPa, a density of 7800 kg/m^3, a Poisson ratio of 0.3, and a thickness of 2 mm. Finally, the displacement and rotation DOFs of the elastic shell are fixed around the edges, and the harmonic analyses are conducted. The obtained pressure responses are compared with those obtained in Matlab® using the transmissibility concept. These pressure responses are also used in the vibro-acoustic source localization routine.

3.2 Experimental Model and Procedure

The experimental setup consists of a wooden box (the same as in [8]) with inner dimensions of 700 mm by 500 mm and 45^o by 100 mm corners. The box is covered with two acrylic plates with thicknesses of 5 mm and 6 mm. In the acoustic setup, the microphones and speakers are placed in holes, at specific coordinates (see table 3.1). A picture of the wooden cavity along with the considered coordinate axes is presented in figure 3.2.

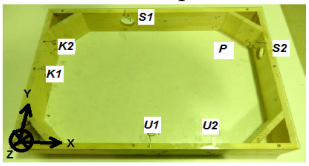

Figure 3.2: Wooden box cavity [8]

.

	x (mm)	y (mm)
$S1$	250	500
$S2$	700	350
$K1$	0	250
$K2$	0	350
$U1$	350	0
$U2$	500	0

Table 3.1: Coordinates of the points of interest in the acoustic cavity [8].

For the vibro-acoustic setup, a steel plate is inserted along $x = 600$ mm, and an excitation is created using a shaker at point P of coordinates $(x, y, z) = (600, 350, 50)$ mm.

The experimental procedure intends to obtain the pressure responses in the cavity over a range of frequencies. In the acoustic experimental setup, a signal is generated in LabVIEW and conveyed to the speakers. The pressure responses are then measured by the microphones and processed in LabVIEW. In the vibro-acoustic setup, an excitation is introduced on the plate (point P), and the pressure responses are measured by the microphones and imported to LabVIEW. The results obtained in these experiments are then compared to the numerical results. The differences between numerical and experimental results dictate how much further updating is needed in the numerical models.

The vibro-acoustic FE model used to analyse the experimental cavity differs from that described in 3.1.3. This model has an higher mesh refinement (0.01 meters of maximum element size), and the plate is only fixed on the edges that are in contact with the wooden box.

3.3 Vibro-Acoustic Source Localization Algorithm

The identification of vibro-acoustic sources is implemented in Matlab® software. A measurement of an arbitrary pressure response in the frequency domain is imported from ANSYS and compared, in Matlab®, with the response obtained at the same node using the transmissibility concept for every possible source. The correct source is the one that minimizes the error function given by

$$\epsilon_{VA} = \sum_{i=1}^{freq} [(P_{meas})_i - (P_{calc})_i]^2 \qquad (3.1)$$

which is a summation along every frequency substep, where P_{meas} is the pressure obtained in ANSYS, P_{calc} is the pressure obtained using the transmissibility concept, and $freq$ is the number of the highest frequency analysed in a given frequency range. The estimated pressure P_{calc} may be expressed as

$$P_{calc} = T_{KU} u_U = H_{UK}^T H_{UU}^{-1} u_U \qquad (3.2)$$

where u_U is the displacement estimation. The displacement estimation matches the sum of the entries in one line of the H_{UU} matrix. For example, if one has two sources, the sum of the first line of the matrix is the displacement at the first source, and the sum of the second line, the displacement at the second source. Yet, this is only valid when there is no

cross-talk. One should also notice that the submatrices of $[H]$ are manipulated in equation 3.2, presenting, therefore, differences between the ones derived in equation 2.18. The way the global matrices are retrieved by ANSYS motivates this manipulation.

3.4 Matlab® Code Optimization

The transmissibility analysis and the problem of source localization usually do not require the entire receptance matrix, but only a few entries. As a consequence, obtaining $[H]$ using the entire inverse of $[Z]$, is quite time consuming and retrieves a considerable amount of unnecessary data. This process may be optimized by obtaining only the necessary entries of $[H]$ using the adjugate matrix and the following equation.

$$[A]^{-1} = (det[A])^{-1} \cdot [adj[A]] \tag{3.3}$$

This is implemented in Matlab® by creating several matrices (one per required entry), and by removing row j and column i of these new matrices. Then, the determinant of these matrices is computed and multiplied by -1 when $i+j$ is an odd number, concluding the derivation of the entries of the adjugate matrix. Finally, one divides these values by the determinant of $[Z]$, and obtains the required entries of $[H]$.

One problem that arises with this method, is that overflow frequently occurs when computing the determinants. This might be solved by multiplying the matrices by a constant and, therefore, change the value of the determinant to fit Matlab®'s precision. However, this method is highly unstable for larger matrices, and in such cases, it may be difficult to implement.

One alternative is to use the logarithm of the determinants. Using LU factorization, the logarithm of the determinant is computed by the summation of the logarithm of every term in the diagonal of $[U]$ (upper triangular matrix). One problem that arises with this method, is that it loses the signal of the determinant. However, the signal may be tracked if one determines the signal of the determinants of $[U]$ and of the permutation matrix $[P]$. The entry of $[H]$ is then computed using

$$H_{ij} = 10^{log(|det[A]|)-log(|det[Z]|)} \tag{3.4}$$

where $[A]$ is the submatrix of $[Z]$ obtained by eliminating row j and column i from $[Z]$.

4 Results and Discussion

In this section are presented the results obtained from applying the methodologies described earlier.

4.1 Mass-spring system

The system in analysis is the MDOF mass-spring system presented in figure 4.1. The mass and stiffness parameters used in the construction of the global matrices are the same as in [2].

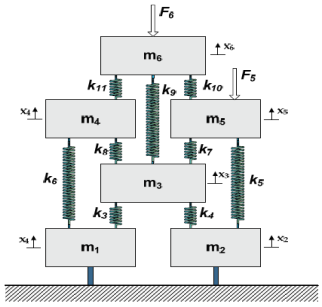

Figure 4.1: MDOF mass-spring system [2].

The transmissibility matrix that relates the coordinates of the supports with the coordinates where the forces are applied is obtained by implementing the methodology described in 3.1.1. The results obtained for the first entry of the transmissibility matrix (T_{15}) are compared with the ones in [2] (figure 4.2).

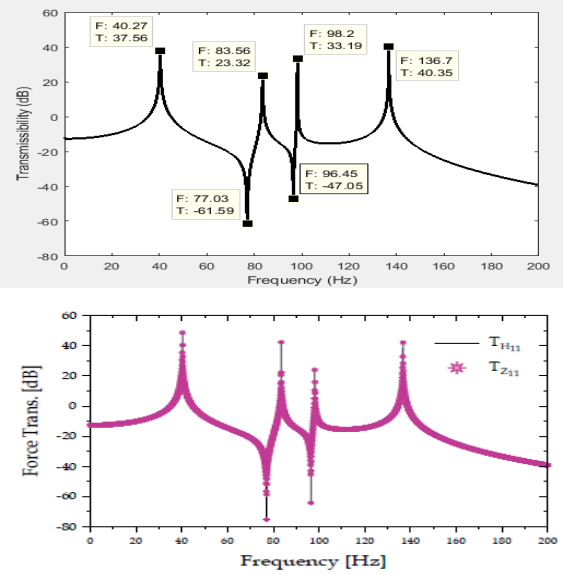

Figure 4.2: Comparison between the obtained results (on the top) and the results in [2] (on the bottom).

It can be observed that the results are similar. However, there are some differences in the amplitudes of the peaks. Such differences are related to the number of frequency substeps considered. In this case, unit substeps are considered. If one used a larger number of substeps, the amplitude differences would be minimized. But the similarities between both results prove that the implemented algorithm is work-

ing properly, and may be extended to the further analyses.

4.2 Acoustic and Vibro-Acoustic Tube

After creating the acoustic tube as described in 3.1.2, a harmonic analysis is created for a frequency of 200 Hz, and the pressure distribution along the length of the tube is obtained. Two cases are considered: the first is of a tube with an imposed pressure of 1 Pa at one end, and a reflective boundary at the other end; the second case has the same imposed pressure, but an anechoic boundary at the second end of the tube. The results obtained along with the analytical solution are presented in figure 4.3, and show that the tube with the reflective boundary requires a higher mesh refinement than the tube with an anechoic boundary. For the tube with the anechoic end, the solution quickly converged to the analytical one, but, in opposition, the solution of the reflective tube, when a mesh of 100 FEs is created (43 elements per wavelength), is still far from the analytical solution. Nevertheless, the results show that the solution is converging to the analytical one with the increasing refinement, proving that the FE model is producing proper results.

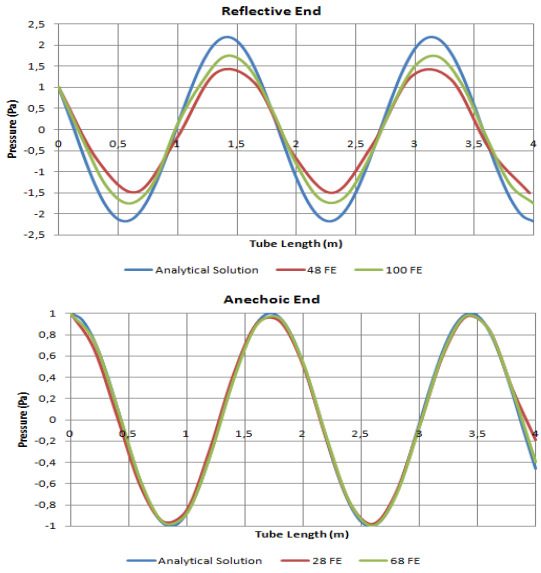

Figure 4.3: Analytical and numerical results for a reflective (top) and an anechoic (bottom) end.

A new FE model is created by dividing a tube in 100 section of 4 elements, creating a centerline along the tube and yielding a total of 909 DOFs and, therefore, 909×909 global matrices. Then, a transmissibility analysis is conducted in Matlab®, and the transmissibility function that relates the node where the pressure is measured (at the mid-section of the tube, along the centerline) with the node where the pressure is imposed (at one end, at the center node) is calculated over a 0 to 500 Hz frequency interval. This is done using the full inverse of $[Z]$ and, alternatively, using the adjugate of $[Z]$ to obtain only the necessary entries of $[H]$. The elapsed and CPU times are compared in table 4.1, proving that using only the necessary entries of $[H]$ requires less computational effort.

Method		Elapsed Time (s)	CPU Time (s)
$[inv[Z]]$	1	424.151	423.933
	2	428.396	427.895
	3	426.517	426.039
$[adj[Z]]$	1	3.688	3.759
	2	3.679	3.713
	3	3.687	3.713

Table 4.1: CPU and elapsed time for an acoustic tube scalar transmissibility analysis.

The vibro-acoustic tube is discretized with 24 elements per wavelength in the longitudinal direction (as in [1]). This model keeps the centerline previously described to introduce the harmonic load at the center of the plate located at the end, and to measure the pressure response at the mid-section. The transmissibility function obtained between these two DOFs is presented in figure 4.4, and shows that the results obtained from the FE model are the same as the results obtained by using vibro-acoustic transmissibility in Matlab®.

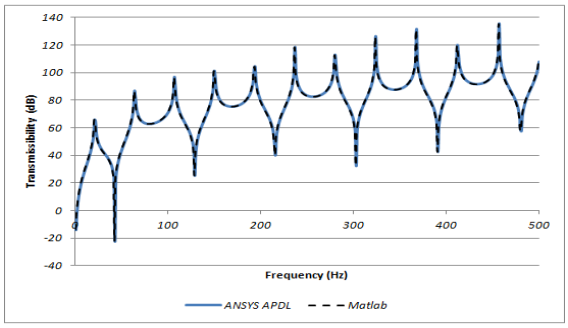

Figure 4.4: Comparison between the results obtained using Matlab®'s transmissibility analysis, and those obtained using the FEM for a vibro-acoustic tube.

Method		Elapsed Time (s)	CPU Time (s)
$[inv[Z]]$	1	48.394	47.564
	2	43.390	43.399
	3	44.061	44.008
$[adj[Z]]$	1	2.072	2.090
	2	2.088	2.153
	3	2.065	2.121

Table 4.2: Simulation times for the transmissibility analysis of a vibro-acoustic tube.

The FE model created has a total of 501 DOFs, and the simulation times required to conduct the transmissibility analysis are presented in table 4.2. Once again, extracting only the necessary entries of $[H]$ proves to be more efficient than using the entire inverse of $[Z]$.

4.3 Acoustic and vibro-acoustic cavities

For the acoustic cavity, a sound signal comprised between 200 and 600 Hz is launched trough the speaker located at $S2$, and the several pressure responses are measured by the microphones at $K1$, $K2$, $U1$ and $U2$.

The results presented in figure 4.6 show that not all the resonances and anti-resonances that appear in the numerical model (see figure 4.5) are present in the experimental results. In addition, there are deviations in frequency between the numerical and experimental resonance peaks. These differences are due to some approximations in the numerical model, such as the fully reflective boundaries, and the 2D model approximation. However, the presence of background noise, interference between electrical wiring and equipment, and non-optimal sensor placement may also be responsible for some of these differences. Nevertheless, the numerical and experimental results share some of the resonances and anti-resonances, proving that the behaviour of the numerical model may be updated to approximate the results.

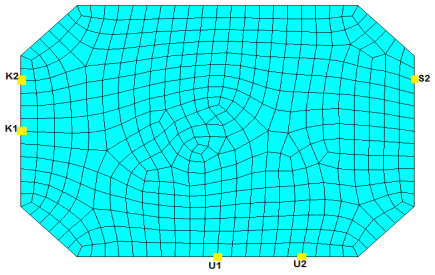

Figure 4.5: Geometry of the modelled acoustic cavity.

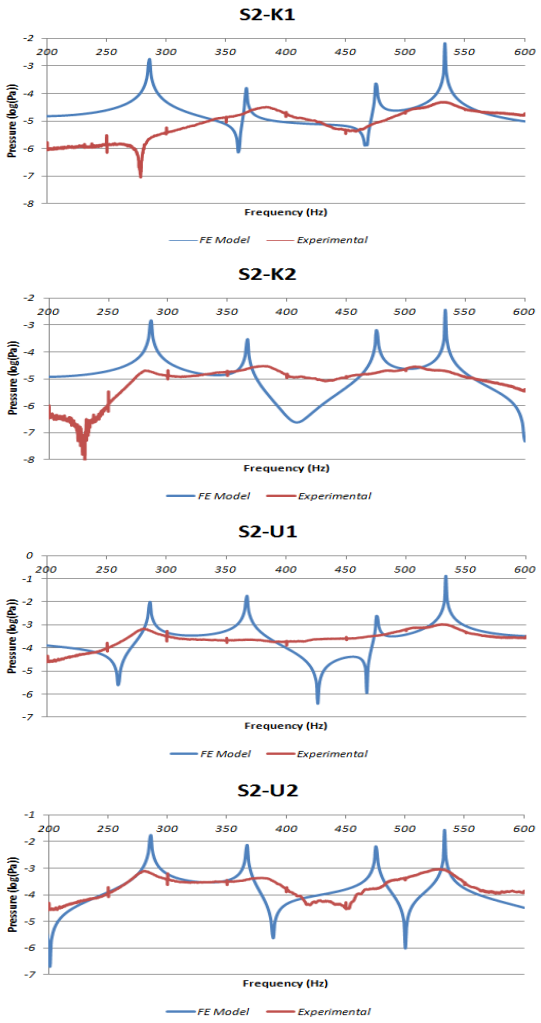

Figure 4.6: Comparison between the numerical and experimental results of the acoustic cavity.

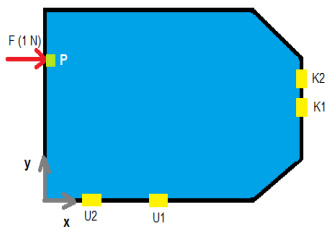

Figure 4.7: Geometry of the modelled vibro-acoustic cavity (cut at Z=50mm).

The numerical model of the vibro-acoustic cavity is used to obtain pressure responses at specific coordinates of the system. These pressure measurements (at $K2$) are then imported to the vibro-acoustic source localization routine. Two cases are considered. First, a case with only one load (source) ap-

plied at point P (cordinates (0;350;50) mm in figure 4.7) (node 259), and a second case with one load at point P and another at the point of the plate with coordinates (0;100,50) mm (with respect to the axes in figure 4.7) (combination 13). The results are obtained with several different levels of added white noise to evaluate the solution robustness.

It can be observed in figure 4.8 that with only one source, despite becoming less prominent with the increasing noise, the minimum remains in the correct node and, as a consequence, the correct source is always identified for the several levels of noise. In the case with two sources, the minimum also becomes less prominent with the increasing noise but, in this case, for a 5% noise addition, the program is no longer able to identify the correct source combination. Nevertheless, it identified the correct sources with lower levels of noise.

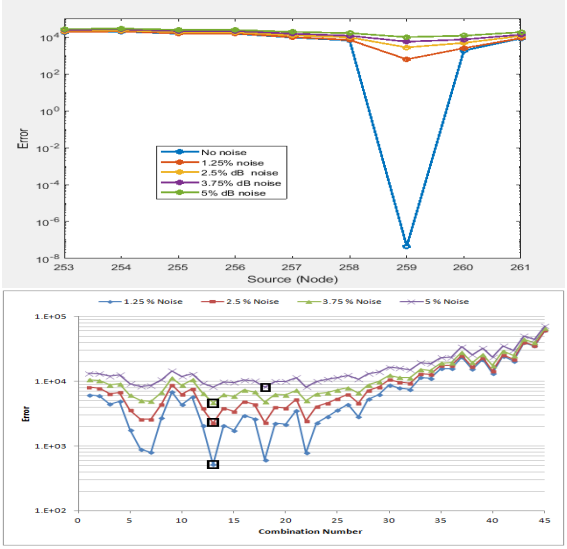

Figure 4.8: Results obtained with the vibro-acoustic source localization routine for 1 (top) and 2 (bottom) sources.

In the vibro-acoustic experimental setup, a swept sin wave from 100 to 700 Hz is applied to the plate and the pressure responses are measured at $K1$, $K2$, $U1$ and $U2$. The results are obtained in LabVIEW between 200 and 600 Hz. These results are presented in figure 4.9 and show, once more, that there are significant differences between the numerical and experimental results. Some of the reasons for these differences were previously mentioned in the analysis of the acoustic cavity. However, in this case, the differences are also due to the vibrations in the wooden box, and to the boundary conditions applied on the steel plate. Since the plate is considered to be fixed on the edges that touch the wooden boards, this boundary is more restrictive than the experimental one (plate fixed by two bolts in each side). This means that, between the numerical and experimental model, there will also be differences in the plate's vibration behaviour, causing differences in the results.

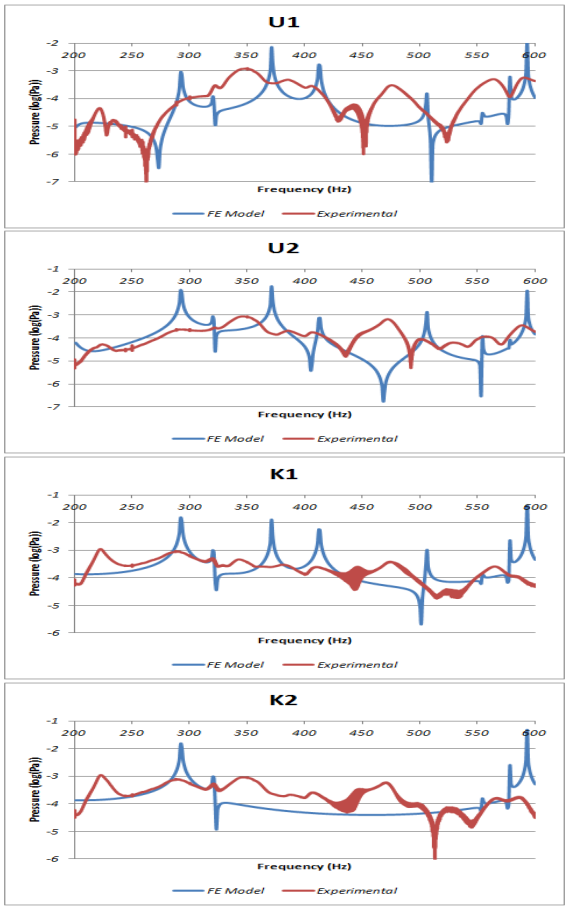

Figure 4.9: Comparison between the numerical and experimental results of the vibro-acoustic cavity.

4.4 Simplified Aircraft Interior Analysis

The main objective of this analysis is to run the vibro-acoustic source localization algorithm in a simplified model of an aircraft.

As the number of possible sources of displacement is quite high in this example, only 123 sources (including the correct one) are studied. Also, to decrease the simulation time, the source identification algorithm is only applied to a parcel of the frequency range. The analysed frequencies are between 35 and 39 Hz, and no noise is added to the pressure measurement obtained at the coordinates (0.75;1.25;1.5) m (see axes in figure 3.1). The results obtained are presented in figure 4.10, and, once again, the minimum occurs in the correct source location, proving that the Matlab® routine is able to accurately iden-

tify the displacement source.

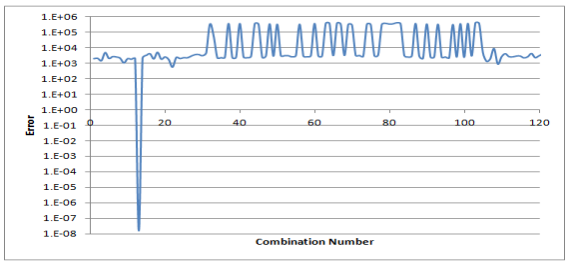

Figure 4.10: Results obtained with the source localization algorithm for the simplified aircraft model.

Usually, the results obtained using the transmissibility concept, match the ones obtained from the FE model. However, this only happens when there is no cross-talk. In the next example, two harmonic loads are applied, one in each vertical wall, as described in 3.1.4. Then, a pressure response is measured at coordinates (0;1.25;1.5) m, and compared with the result obtained using the transmissibility concept.

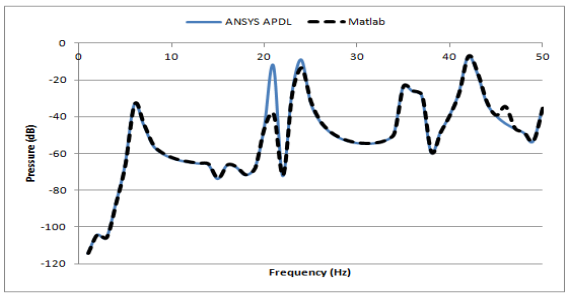

Figure 4.11: Comparison between the results obtained using ANSYS harmonic analysis and using multi-point transmissibility analysis in Matlab®.

As it can be observed in figure 4.11, there are differences between the results produced with the two models. These differences only appear around a few frequency intervals, and are related to the existence of cross-talk between the two sources.

5 Conclusions

This work "proves" that the transmissibility concept may be applied to the estimation of pressure responses in vibro-acoustic systems, and to the identification of vibro-acoustic sources. However, the vibro-acoustic source localization routine continues to demand large simulation times for larger models, even with the advances presented in terms of reducing the computational effort. Nevertheless, the simplicity of the proposed solutions make this concept quite promising for OTPA.

Future developments in this area may include the study of cross-talk cancellation, further updating in the numerical and experimental models, and developing methodologies to study transmissibility functions using a combined approach between Statistical Energy Analysis and the MDOF transmissibility concept.

References

[1] V. M. N. Martins. Estimating Vibration, Acoustic and Vibro-Acoustic responses using Transmissibility functions. Master Thesis, Instituto Superior Técnico, 2019.

[2] N. M. M. Maia, A. P. V. Urgueira, and R. A. B. Almeida. Whys and Wherefores of Transmissibility. In D. F. Beltran-Carbajal, editor, *Vibration Analysis and Control - New Trends and Developments*, chapter 10, Pages 187-216, ISBN 978-953-307-433-7, September 2011.

[3] M. M. Neves and N. M. M. Maia. Estimation Of Applied Force Using The Transmissibility Concept. *Proceedings of ISMA2010 Including USD2010*, Pages 3887-3898, 2010.

[4] Y. E. Lage, M. M. Neves, N. M. M. Maia, and D. Tcherniak. Force transmissibility versus displacement transmissibility. *Journal of Sound and Vibration*, Pages 5708-5722, ISSN 10958568, DOI: 10.1016/j.jsv.2014.05.038, 2014.

[5] C. D. V. Guedes. Localização de Fontes Acústicas em Interiores de Avião Usando o Conceito de Transmissibilidade. Master Thesis (In Portuguese), Instituto Superior Técnico, 2016.

[6] Theory Reference for the Mechanical APDL and Mechanical Applications. 3304(April):724-746, 2009.

[7] M. M. Neves, H. F. D. Policarpo, N. M. M. Maia, D. Tcherniak. A note on the use of vibro-acoustic transmissibility to estimate vibro-acoustic responses. Proceedings of the ICEDyn, Viana do Castelo, 2019.

[8] H. F. D. Policarpo. Experimental and numerical acoustic and vibro-acoustic characterization of a wooden cavity. Technical Report September, Instituto Superior Técnico, Lisbon, Portugal, 2017.

[9] F. J. P. Lau. Elementos de Aeroacústica. 2017.

[10] W. Desmet, D.Vandepitte. Finite Element Method in Acoustics. Proceedings of the ISAAC13, ISBN 90-73802-73-3, 2002.

[11] A. J. F. Cartaxo. Caracterização de Filtros Acústicos Baseada no Método dos Elementos Finitos. Master Thesis (In Portuguese), Instituto Superior Técnico, 2007.

[12] C.Howard. Coupled Structural-Acoustic Analysis Using ANSYS. Internal Report, The University of Adelaide, Department of Mechanical Engineering, Pages 1-15, 2000.